MATERIAL SCIENCE / МАТЕРИАЛОВЕДЕНИЕ

UDC 536.425:539.25:539.351
DOI 10.17073/0368-0797-2023-4-427-433

Original article
Оригинальная статья

Structure and properties of HEA surface layer after electron-ion-plasma processing

Yu. F. Ivanov[1], V. V. Shugurov[1], A. D. Teresov[1], E. A. Petrikova[1], M. O. Efimov[2]

[1] **Institute of High Current Electronics, Siberian Branch of the Russian Academy of Sciences** (2/3 Akademicheskii Ave., Tomsk 634055, Russian Federation)
[2] **Siberian State Industrial University** (42 Kirova Str., Novokuznetsk, Kemerovo Region – Kuzbass 654007, Russian Federation)

yufi55@mail.ru

Abstract. High-entropy alloys (HEAs) are the most actively researched materials of recent decades. In the present work, the non-equiatomic AlCrFeCoNi wind turbine is manufactured using cold metal transfer technology and investigated by the methods of modern physical materials science. The authors analyzed the elemental and phase compositions, defective substructure and tribological properties of the HEA surface layer formed as a result of complex processing, which combines the deposition of a film (B + Cr) and irradiation with a pulsed electron beam in an argon medium. In the initial state, the alloy has a simple cubic lattice with a lattice parameter of 0.28795 μm, the average grain size of the HEA is 12.3 μm. Chemical composition of the HEA is as follows, at. %: 33.4 Al; 8.3 Cr; 17.1 Fe; 5.4 Co; 35.7 Ni. The elements are distributed quasi-periodically. The irradiation mode was revealed (electron-beam energy density 20 J/cm^2; irradiation duration 200 μs, number of pulses 3; pulse frequency 0.3 s^{-1}), which allows to increase microhardness (almost twice) and wear resistance (more than by five times), to reduce the friction coefficient by 1.3 times. At an electron-beam energy density of 20 J/cm^2, the surface is fragmented by a grid of microcracks. Size of the fragments varies between 40 – 200 μm. An increase in the electron-beam energy density leads to complete dissolution of the film (B + Cr). Regardless of the magnitude of the electron-beam energy density, the wind turbine is a single-phase material and has a simple cubic crystal lattice. High-speed crystallization of the surface layer leads to the formation of a subgrain structure (150 – 200 nm). It is suggested that an increase in the strength and tribological properties of wind turbines is due to a significant (by 4.5 times) decrease in the average grain size, formation of chromium and aluminum oxide particles, and introduction of boron atoms into the crystal lattice of wind turbines.

Keywords: high-entropy alloy, cold metal transfer technology, film/substrate system, electron-ion-plasma processing, elemental and phase composition, defect structure

Acknowledgements: The work was supported by the Russian Science Foundation (project No. 19-19-00183 – modification of HEA, study of the structure and properties of the modified HEA layer; and project No. 20-19-00452 – production of HEA samples using cold metal transfer technology).

For citation: Ivanov Yu. F., Shugurov V.V., Teresov A.D., Petrikova E.A., Efimov M.O. Structure and properties of HEA surface layer after electron-ion-plasma processing. *Izvestiya. Ferrous Metallurgy*. 2023;66(4):427–433. https://doi.org/10.17073/0368-0797-2023-4-427-433

Структура и свойства поверхностного слоя ВЭС после электронно-ионно-плазменной обработки

Ю. Ф. Иванов[1], В. В. Шугуров[1], А. Д. Тересов[1], Е. А. Петрикова[1], М. О. Ефимов[2]

[1] **Институт сильноточной электроники Сибирского отделения РАН** (Россия, 634055, Томск, пр. Академический, 2/3)
[2] **Сибирский государственный индустриальный университет** (Россия, 654007, Кемеровская обл. – Кузбасс, Новокузнецк, ул. Кирова, 42)

yufi55@mail.ru

Аннотация. Высокоэнтропийные сплавы (ВЭС) являются наиболее активно исследуемыми материалами последних десятилетий. В настоящей работе ВЭС неэквиатомного состава AlCrFeCoNi изготовлен по технологии холодного переноса металла и исследован методами современного физического материаловедения. Выполнен анализ элементного и фазового составов, дефектной субструктуры и трибологических свойств поверхностного слоя ВЭС, сформированного в результате комплексной обработки, которая сочетает напыление пленки (B + Cr) и облучение импульсным электронным пучком в среде аргона. В исходном состоянии сплав имеет простую кубическую

решетку с параметром 0,28795 мкм, средний размер зерна ВЭС составляет 12,3 мкм. Химический состав: 33,4 % Al; 8,3 % Cr; 17,1 % Fe; 5,4 % Co; 35,7 % Ni (ат.). Элементы распределены квазипериодически. Выявлен режим облучения (плотность энергии пучка электронов 20 Дж/см^2; длительность облучения 200 мкс, количество импульсов 3; частота импульсов 0,3 с$^{-1}$), который позволяет повысить микротвердость (почти в два раза) и износостойкость (более чем в пять раз), снизить коэффициент трения в 1,3 раза. При плотности энергии пучка электронов 20 Дж/см^2 поверхность фрагментируется сеткой микротрещин. Размеры фрагментов изменяются в пределах 40 – 200 мкм. Увеличение плотности энергии пучка электронов приводит к полному растворению пленки (B + Cr). Независимо от величины плотности энергии пучка электронов ВЭС является однофазным материалом, имеет простую кубическую кристаллическую решетку. Высокоскоростная кристаллизация поверхностного слоя приводит к формированию субзеренной структуры (150 – 200 нм). Высказывается предположение, что увеличение прочностных и трибологических свойств ВЭС обусловлено существенным (в 4,5 раза) снижением среднего размера зерна, формированием частиц оксиборидов хрома и алюминия, внедрением атомов бора в кристаллическую решетку ВЭС.

Ключевые слова: высокоэнтропийный сплав, технология холодного переноса металла, система пленка/подложка, электронно-ионно-плазменная обработка, элементный и фазовый состав, дефектная структура

Благодарности: Работа выполнена за счет гранта Российского научного фонда (проект № 19-19-00183), https://rscf.ru/project/19-19-00183/ – модифицирование ВЭС, исследование структуры и свойств модифицированного слоя ВЭС; при финансовой поддержке гранта Российского научного фонда (проект № 20-19-00452) – изготовление образцов ВЭС с помощью технологии холодного переноса металла.

Для цитирования: Иванов Ю.Ф., Шугуров В.В., Тересов А.Д., Петрикова Е.А., Ефимов М.О. Структура и свойства поверхностного слоя ВЭС после электронно-ионно-плазменной обработки. *Известия вузов. Черная металлургия*. 2023;66(4):427–433. https://doi.org/10.17073/0368-0797-2023-4-427-433

Introduction

The development and study of high-entropy alloys (HEAs) are of significant scientific interest due to their unique microstructure [1; 2], composite composition [3], and mechanical properties [4 – 6]. In contrast to traditional alloys, which typically consist of one or two basic elements, HEAs are composed of several major elements (at least five) in equimolar or near-equimolar ratios. The original findings in the field of HEAs are extensively discussed in analytical reviews [7 – 9] and monographs (e.g., [10]). These publications describe the microstructure, properties, and thermodynamics, review the results of structural modeling, and explore novel methods for producing multi-component alloys. Substantial efforts have been dedicated to addressing the challenge of enhancing the mechanical properties of five-component alloys like MnCoCrFeNi and AlCoCrFeNi through grain boundary strengthening [11; 12], solid solution hardening [13 – 16], and interstitial solid-solution hardening [17]. Relevant theoretical developments are also in progress [18]. The paper [13] proposes a method to enhance strength through partial amorphization, as this structure lacks grain boundaries or dislocations. To improve surface properties, HEAs undergo various types of surface treatments. For example, the paper [19] reviews various processing methods and their impact on the surface of CoCrFeMnNi HEA obtained through selective laser melting. The considered treatments include electrolytic polishing, electro-erosion machining, milling, grinding, mechanical polishing with abrasives, and combinations of these methods. The results demonstrate that grinding smoothes the surface and increases microhardness, however, it leaves tool marks and residual stresses due to microstructure deformation. Mechanical polishing using abrasives enables the creation of an ultra-smooth surface without subsurface damage. Electro-erosion machining results in surface melting, leading to increased residual stresses and microhardness. When electrolytic polishing is combined with other methods, it removes residual stresses and damage caused by previous processing, thereby smoothing the surface. However, when electrolytic polishing is used in isolation from other methods, a micrometer-level surface roughness cannot be achieved. The paper [20] addresses the challenge of low strength and wear resistance in the CoCrFeMnNi alloy with an FCC crystal lattice by employing the powder-pack boriding method. This treatment results in a double layer enriched with silicon and boron, leading to increased microhardness and wear resistance in the borated samples. One of the most promising and highly efficient methods for surface hardening is electron-beam treatment [9; 10]. This treatment ensures ultrahigh heating rates of the surface layer (up to 10^6 K/s) to the specified temperatures, followed by cooling rates of $10^4 – 10^9$ K/s through heat extraction into the bulk of the material. As a result, non-equilibrium submicro- and nanocrystalline structural-phase states emerge in the surface layer.

The aim of this research is to analyze the elemental and phase compositions, as well as the defect substructure of the HEA surface layer formed as a result of complex treatment, combining film deposition (B + Cr) and pulsed electron beam irradiation.

Materials and methods

The study material utilized was a HEA with the elemental composition AlCrFeCoNi, which was obtained using cold metal transfer technology [20]. The samples had dimensions of 15×15×5 mm. The surface treatment of the HEA samples was carried out in two steps: *1* – formation of a "film/substrate" system: a 0.5 μm thick boron film was deposited, and on top of it, a 0.5 μm thick chromium film was added; *2* – irradiation of the "film (B) + film (Cr)/HEA (substrate)" system with a pulsed electron beam.

The boron film was deposited onto the surface of HEA samples using plasma-assisted radio frequency sputtering (RF sputtering) of boron powder cathode. The following process parameters were applied: power $W = 800$ W; frequency $f = 13.56$ MHz; duration of processes $t = 35$ min (resulting in a 0.5 μm thick boron film); current of PINK plasma generator $I_p = 50$ A; heating current $I_h = 145$ A; bias voltage $U_b = 50$ V; duty cycle 75 %; bias frequency 50 kHz. Before applying the boron film, the surface of the HEA samples, following placement in the installation chamber and subsequent evacuation, underwent a brief 15-minute etching process with argon plasma. The 0.5 μm thick chromium film was deposited onto the samples with the boron film using an arc evaporator. The following process parameters were employed: samples with the boron film were placed opposite the arc evaporator, without rotation; arc evaporator current $I_a = 80$ A; plasma generator current $I_p = 20$ A; heating current $I_h = 135$ A; duty cycle 75 %; bias voltage $U_b = 35$ V; pressure $p = 0.3$ Pa; chromium deposition $t = 10$ min. The "film/substrate" system was then irradiated with an intense pulsed electron beam on the SOLO installation, employing the following process parameters: energy of accelerated electrons is 18 keV, energy density of the electron beam is 20 – 40 J/cm^2; pulse duration is 200 μs; number of pulses is 3; pulse repetition rate is 0.3 s^{-1}; pressure of the working gas (argon) is 0.02 Pa. Based on estimations [10], under these irradiation parameters, the temperature of the surface layer of the "film (B + Cr)/(HEA) substrate" system surpasses the melting point of the HEA. This leads to the expectation that the process of forming a molten surface layer of HEA samples alloyed with boron and chromium atoms (during rapid heating) and the subsequent development of a submicro- and nanocrystalline multiphase structure strengthened with metal borides (during rapid cooling) will occur.

The phase composition and the condition of the crystal lattice in the main phases of the sample's surface layer were investigated through *X*-ray phase and *X*-ray diffraction analysis. This analysis was conducted using a Shimadzu XRD 6000 *X*-ray diffractometer located in Kyoto, Japan. *X*-ray shooting utilized copper-filtered Cu$K_{\alpha 1}$ radiation and a CM-3121 monochromator. The phase composition was determined with reference to the PDF 4+ databases, and full-profile analysis was performed using the POWDER CELL 2.4 program. To achieve the desired film thickness, the deposition modes for the boron and chromium films were selected through experiments employing the Calotest CAT-S-0000 device, designed to determine film thickness. Material hardness was assessed using the Vickers method on a PMT-3 microhardness tester with a 0.5 N load. The tribological characteristics, including the friction coefficient and wear parameter of the material, were examined using a Pin on Disc and Oscillating TRIBOtester tribometer by TRIBOtechnic in Clichy, France. The tests were conducted with a ceramic Al_2O_3 ball, 6 mm in diameter, a 2 mm radius for the friction track, a 100 m path for the counter body's travel, a sample rotation speed of 25 mm/s, and an indenter load of 2 N. These tribological tests were performed under dry friction conditions at room temperature.

Results and discussion

The HEA produced through additive technology exhibits a dendritic structure. Dendrites are polycrystalline aggregates with an average grain size of 12.3 μm. *X*-ray microanalysis revealed that the HEA consists of the chemical elements Al, Cr, Fe, Co, and Ni in the following proportions at. %: Al 33.4; Cr 8.3; Fe 17.1; Co 5.4; Ni 35.7.

A mapping technique was employed to visualize the distribution of atoms within the alloy's bulk. The results indicate that the boundaries of grains and dendrites are enriched with chromium and iron atoms, while the volume of the grains contains higher concentrations of aluminum and nickel. Cobalt atoms are distributed in a quasi-homogeneous manner throughout the alloy's bulk.

X-ray phase analysis confirmed that the alloy in question possesses a simple cubic crystal lattice, with a crystal lattice parameter is 0.28795 nm.

Irradiation of the "film/substrate" system with a pulsed electron beam induces significant alterations in the mechanical and tribological properties of HEA samples. Firstly, there is a substantial increase in microhardness, with the maximum value achieved following irradiation of the "film/substrate" system with a pulsed electron beam having an electron beam energy density (E_s) of 20 J/cm^2 (Fig. 1, *a*). Secondly, the wear resistance of the samples improves, and the friction coefficient decreases, with the most favorable outcomes observed after irradiation of the "film/substrate" system with a pulsed electron beam having an energy density of 20 J/cm^2 (Fig. 1, *b*, *c*).

The alterations in the mechanical and tribological properties of the alloy are evidently attributed to changes in the structure of the surface layer of the samples. It was observed that when the "film/substrate" system is exposed to an electron beam with an energy density of 20 J/cm^2, the sample's surface undergoes fragmentation, forming a network of microcracks (Fig. 2, *a*). These microcracks vary in size from 40 to 200 μm, with an average size of 104 μm. Within the fragments, a grain structure becomes apparent (Fig. 2, *c*). The average grain size within the fragments measures 2.7 μm, which is 4.5 times smaller than the average grain size of the initial HEA.

With an increase in electron beam energy density, the average grain size of the HEA surface layer also increases, reaching 19 μm when $E_s = 40$ J/cm^2. it reaches 19 μm. It is evident that the significant reduction in the average grain size of the surface layer when

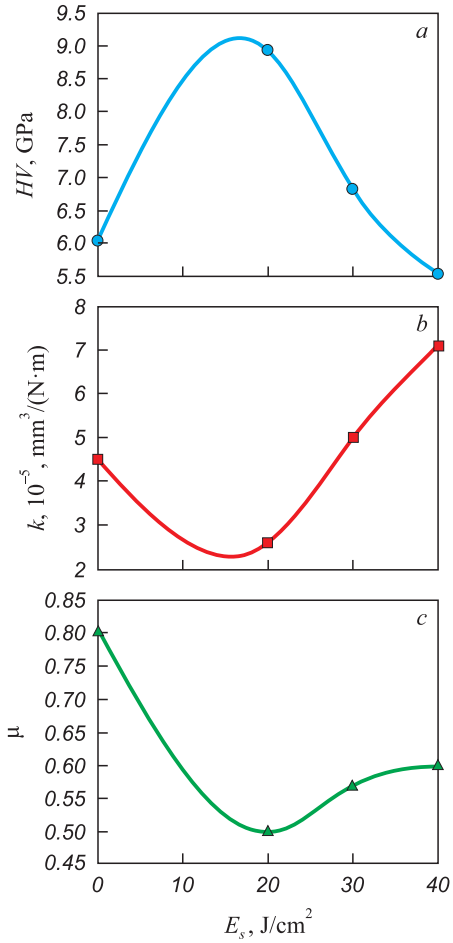

Fig. 1. Dependence of microhardness (*a*), wear parameter (*b*) and friction coefficient (*c*) of the film/substrate system surface layer on electron-beam energy density. In the initial state of wind turbine (without a sprayed film and irradiation), microhardness is 4.7 GPa, wear parameter is $14 \cdot 10^{-5}$ mm^3/(N·m), friction coefficient is 0.65

Рис. 1. Зависимость микротвердости (*a*), параметра износа (*b*) и коэффициента трения (*c*) поверхностного слоя системы «пленка/подложка» от плотности энергии пучка электронов. В исходном состоянии ВЭС (без напыленной пленки и без облучения) микротвердость 4,7 ГПа, параметр износа $14 \cdot 10^{-5}$ мм^3/(Н·м), коэффициент трения 0,65

$E_s = 20$ J/cm^2 is one of the reasons for the improvement in the alloy's strength properties, a phenomenon known as the Hall–Petch effect.

Irradiation of the "film/substrate" system with a pulsed electron beam at $E_s = 20$ J/cm^2 does not result to the complete dissolution of the film. Instead, we observe extended film interlayers within the bulk and along the boundaries of the fragments, as well as film islands situated at the junctions of the fragments (Fig. 2, *b*, *c*).

With the increase in electron beam energy density, reaching 30 J/cm^2 and subsequently 40 J/cm^2, the (B + Cr) film completely dissolves (Fig. 3). In these cases, the surface of the samples is once again fragmented by a network of microcracks, which signifies the formation of significant tensile stresses within the surface layer of the alloy as it is irradiated.

The rapid solidification of the surface layer results in the creation of a sub-grain structure, often referred to as a rapid solidification structure (Fig. 3, *c*). When $E_s = 20$ J/cm^2, the subgrain structure is infrequently observed, at $E_s = 30$ J/cm^2, it forms at the junctions of grain boundaries and fragments; and at $E_s = 40$ J/cm^2, subgrains are formed across the entire surface of the sample. The size of these subgrains remains consistent and ranges from 150 to 200 nm, independent of the energy density of the electron beam.

X-ray microanalysis was employed to demonstrate that the sections of the film that remain after irradiation of the "film/substrate" system with a pulsed elec-

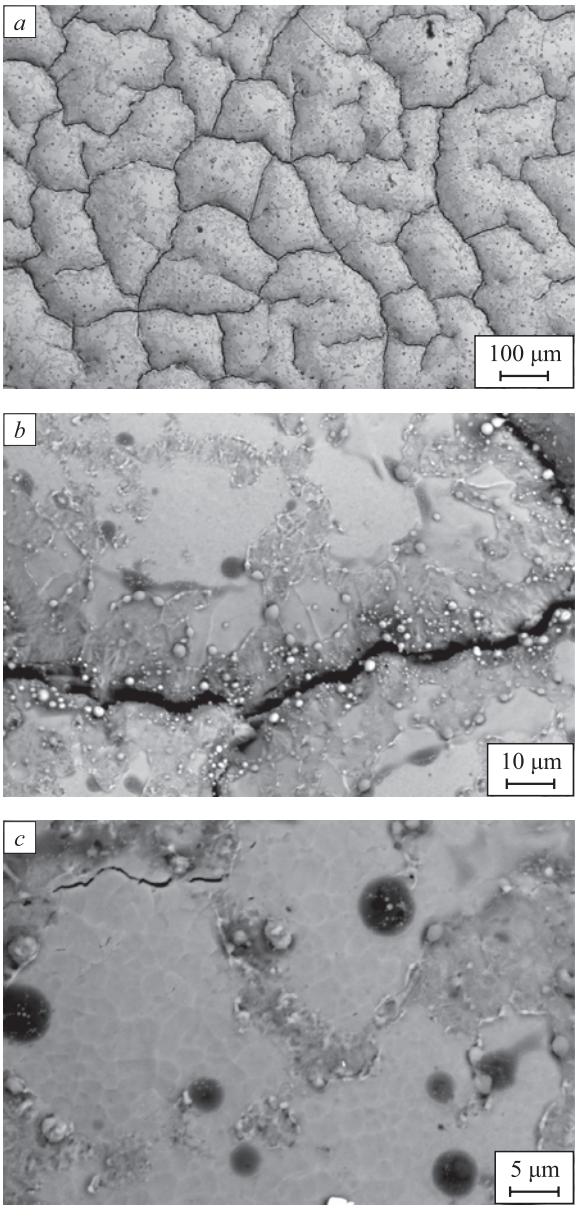

Fig. 2. Structure of the film/substrate system irradiated by a pulsed electron beam at energy density of 20 J/cm^2

Рис. 2. Структура системы «пленка/подложка», облученной импульсным электронным пучком при плотности энергии пучка электронов 20 Дж/см^2

tron beam at 20 J/cm^2 are enriched with chromium, boron, and oxygen atoms.

Additionally, extended interlayers along the fragment boundaries are observed to be enriched with oxygen and aluminum.

The islands that form on the HEA surface when the "film/substrate" system is irradiated with an electron beam, with an energy density of 30 and 40 J/cm^2, are found to be enriched with chromium, aluminum, and oxygen atoms. This indicates that, as a result of irradiation of the "film/substrate" system with a pulsed electron beam, chromium and aluminum oxiborides are formed on the HEA surface. The quantity of these oxiborides decreases as the energy density of the electron beam increases. The formation of oxiborides contributes to the enhancement of HEA microhardness and wear resistance.

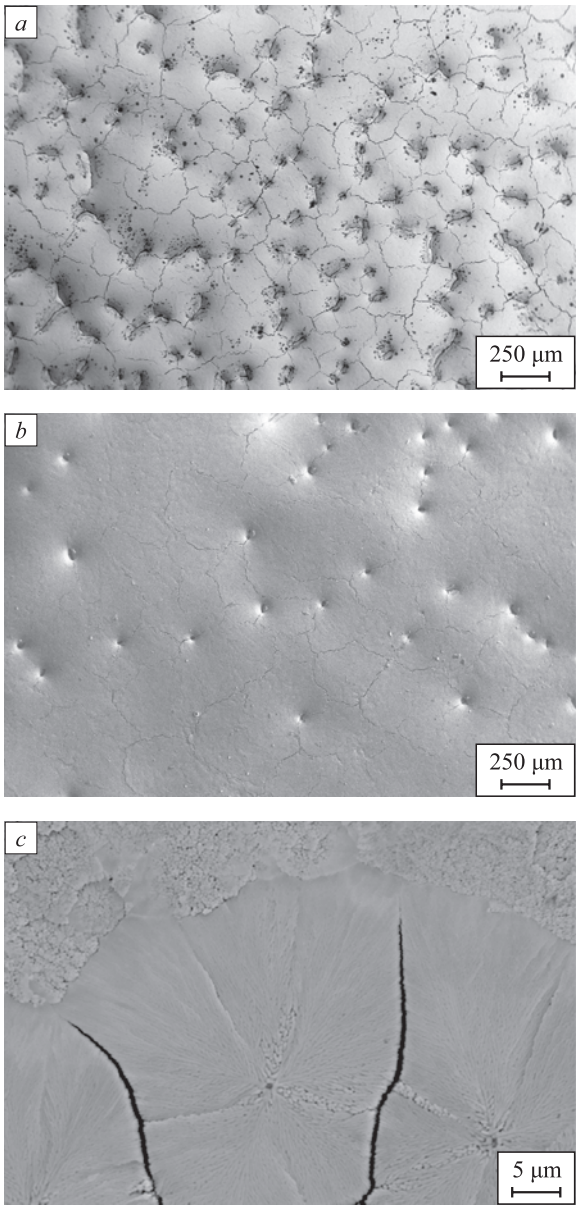

Fig. 3. Structure of the film/substrate system irradiated by a pulsed electron beam at energy density of 30 J/cm^2 (*a*) and 40 J/cm^2 (*b*, *c*)

Рис. 3. Структура системы «пленка/подложка», облученной импульсным электронным пучком при плотности энергии пучка электронов 30 Дж/см^2 (*a*) и 40 Дж/см^2 (*b*, *c*)

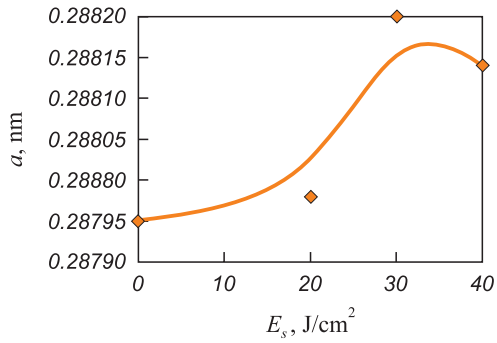

Fig. 4. Dependence of crystal lattice parameter of the film/substrate system surface layer on electron beam energy density

Рис. 4. Зависимость параметра кристаллической решетки поверхностного слоя системы «пленка/подложка» от плотности энергии пучка электронов

The phase composition of the HEA surface layer, modified due to irradiation of the "film/substrate" system with a pulsed electron beam, was investigated through *X*-ray phase analysis. Regardless of the value of E_s, the alloy remains a single-phase material with a simple cubic crystal lattice.

The lattice parameter exhibits an ambivalent dependence on the value of E_s (Fig. 4). One of the reasons for the variation in the crystal lattice parameter of the alloy is the incorporation of boron atoms into the samples, and their concentration within the bulk of the alloy increases as the energy density falls within the range $E_s = (20 – 30)$ J/cm^2. It is worth noting that the boron atoms within the HEA crystal lattice will occupy interstitial positions, leading to an increase in the lattice parameter. The formation of a solid interstitial solution is another physical mechanism contributing to the hardness of the alloy. The absence of detectable strengthening phases in the alloy under study by *X*-ray phase analysis may be attributed to their limited quantity.

Conclusions

HEA samples with non-equiatomic elemental composition AlCrFeCoNi were manufactured using cold metal transfer technology. A comprehensive treatment of the HEA samples' surface layer was carried out, combining the creation of the "film (Cr + B)/(HEA) substrate" system with subsequent irradiation using a pulsed electron beam at various electron beam energy density levels (ranging from 20 – 40 J/cm^2. The optimized irradiation mode (electron-beam energy density of 20 J/cm^2, irradiation duration of 200 μs, three pulses, pulse frequency of 0.3 s^{-1}) was identified, resulting in a significant increase in microhardness (almost double), enhanced wear

resistance (over fivefold improvement), and a 1.3-fold reduction in the friction coefficient. The conducted studies of the structure and phase composition suggested that the improvement in HEA strength and tribological properties is linked to a considerable reduction in average grain size (4.5 times smaller), the formation of chromium and aluminum oxyboride particles, and the incorporation of boron atoms into the HEA crystal lattice.

References / Список литературы

1. Shivam V., Basu J., Pandey V.K., Shadangi Y., Mukhopadhyay N.K. Alloying behaviour, thermal stability and phase evolution in quinary AlCoCrFeNi high entropy alloy. *Advanced Powder Technology*. 2018;29(9):2221–2230. https://doi.org/10.1016/j.apt.2018.06.006
2. Alshataif Y.A., Sivasankaran S., Al-Mufadi F.A., Alaboodi A.S., Ammar H.R. Manufacturing methods, microstructural and properties evolutions of high-entropy alloy: A review. *Metals and Materials International*. 2020;26:1099–1133. https://doi.org/10.1007/s12540-019-00565-z
3. Ganesh U.L., Raghavendra H. Review on the transition from conventional to multicomponent-based nano-high-entropy alloys-NHEAs. *Journal of Thermal Analysis and Calorimetry*. 2020;139:207–216. https://doi.org/10.1007/s10973-019-08360-z
4. George E.P., Curtin W.A., Tasan C.C. High entropy alloys: A focused review of mechanical properties and deformation mechanisms. *Acta Materialia*. 2020;188:435–474. https://doi.org/10.1016/j.actamat.2019.12.015
5. Cheng K.C., Chen J.H., Stadler S., Chen S.H. Properties of atomized AlCoCrFeNi high-entropy alloy powders and their phase-adjustable coatings prepared via plasma spray process. *Applied Surface Science*. 2019;478:478–486. https://doi.org/10.1016/j.apsusc.2019.01.203
6. Miracle D.B., Senkov O.N. A critical review of high entropy alloys and related concepts. *Acta Materialia*. 2017;122:448–511. https://doi.org/10.1016/j.actamat.2016.08.081
7. Zhang W., Liaw P.K., Zhang Y. Science and technology in high-entropy alloys. *Science China Materials*. 2018;61(1):2–22. https://doi.org/10.1007/s40843-017-9195-8
8. Osintsev K.A., Gromov V.E., Konovalov S.V., Ivanov Yu.F., Panchenko I.A. High-entropy alloys: Structure, mechanical properties, deformation mechanisms and application. *Izvestiya. Ferrous Metallurgy*. 2021;64(4):249–258. https://doi.org/10.17073/0368-0797-2021-4-249-258

   Осинцев К.А., Громов В.Е., Коновалов С.В., Иванов Ю.Ф., Панченко И.А. Высокоэнтропийные сплавы: структура, механические свойства, механизмы деформации и применение. *Известия вузов. Черная металлургия*. 2021;64(4):249–258. https://doi.org/10.17073/0368-0797-2021-4-249-258
9. Ivanov Yu.F., Gromov V.E., Zagulyaev D.V., Konovalov S.V., Rubannikova Yu.A., Semin A.P. Prospects for the application of surface treatment of alloys electron beams in state of the art technologies. *Progress in Physics of metals*. 2020;21(3):345–362. https://doi.org/10.15407/ufm.21.03.345

   Иванов Ю.Ф., Громов В.Е., Загуляев Д.В., Коновалов С.В., Рубанникова Ю.А., Семин А.П. Перспективы применения поверхностной обработки сплавов электронными пучками в современных технологиях. *Успехи физики металлов*. 2020;21(3):345–362. https://doi.org/10.15407/ufm.21.03.345
10. Gromov V.E., Konovalov S.V., Osintsev K.A. *Structure and Properties of High Entropy Alloys*. Springer; 2021;110.
11. Wu Z., Bei H., Pharr G.M., George E.P. Temperature dependence of the mechanical properties of equiatomic solid solution alloys with face-centered cubic crystal structures. *Acta Materialia*. 2014;81:428–441. https://doi.org/10.1016/j.actamat.2014.08.026
12. Schuh B., Mendez-Martin F., Völker B., George E.P., Clemens H., Pippan R., Hohenwarter A. Mechanical properties, microstructure and thermal stability of a nanocrystalline CoCrFeMnNi high-entropy alloy after severe plastic deformation. *Acta Materialia*. 2015;96:258–268. https://doi.org/10.1016/j.actamat.2015.06.025
13. Gali A., George E.P. Tensile properties of high- and medium-entropy alloys. *Intermetallics*. 2013;39:74–78. https://doi.org/10.1016/j.intermet.2013.03.018
14. Li Z., Tasan C.C., Springer H., Gault B., Raabe D. Interstitial atoms enable joint twinning and transformation induced plasticity in strong and ductile high-entropy alloys. *Scientific Reports*. 2017;7:40704. https://doi.org/10.1038/srep40704
15. Xiao L.L., Zheng Z.Q., Guo S.W., Huang P., Wang F. Ultrastrong nanostructured CrMnFeCoNi high entropy alloys. *Materials and Design*. 2020;194:108895. https://doi.org/10.1016/j.matdes.2020.108895
16. Coury F.G., Kaufman M., Clarke A.J. Solid-solution strengthening in refractory high entropy alloys. *Acta Materialia*. 2019;175:66–81. https://doi.org/10.1016/j.actamat.2019.06.006
17. Ikeda Y., Tanaka I., Neugebauer J., Körmann F. Impact of interstitial C on phase stability and stacking-fault energy of the CrMnFeCoNi high-entropy alloy. *Physical Review Materials*. 2019;3(11):113603. https://doi.org/10.1103/PhysRevMaterials.3.113603
18. Laplanche G., Kostka A., Horst O.M., Eggeler G., George E.P. Microstructure evolution and critical stress for twinning in the CrMnFeCoNi high-entropy alloy. *Acta Materialia*. 2016;118:152–163. https://doi.org/10.1016/j.actamat.2016.07.038
19. Guo J., Goh M., Zhu Z., Lee X., Nai M.L.S., Wei J. On the machining of selective laser melting CoCrFeMnNi high-entropy alloy. *Materials and Design*. 2018;153:211–220. https://doi.org/10.1016/j.matdes.2018.05.012
20. Lindner T., Löbel M., Sattler B., Lampke T. Surface hardening of FCC phase high-entropy alloy system by powder-pack boriding. *Surface and Coatings Technology*. 2019;371:389–394. https://doi.org/10.1016/j.surfcoat.2018.10.017

Information about the Authors

Yurii F. Ivanov, *Dr. Sci. (Phys.-Math.), Prof., Chief Researcher of the Laboratory of Plasma Emission Electronics,* Institute of High-Current Electronics, Siberian Branch of the Russian Academy of Sciences
ORCID: 0000-0001-8022-7958
E-mail: yufi55@mail.ru

Vladimir V. Shugurov, *Research Associate of the Laboratory of Plasma Emission Electronics,* Institute of High-Current Electronics, Siberian Branch of the Russian Academy of Sciences
ORCID: 0000-0001-6148-9442
E-mail: shugurov@inbox.ru

Anton D. Teresov, *Senior Researcher of the Laboratory of Plasma Emission Electronics,* Institute of High-Current Electronics, Siberian Branch of the Russian Academy of Sciences
ORCID: 0000-0002-5363-0108
E-mail: tad514@sibmail.com

Elizaveta A. Petrikova, *Junior Researcher of the Laboratory of Plasma Emission Electronics,* Institute of High-Current Electronics, Siberian Branch of the Russian Academy of Sciences
ORCID: 0000-0002-1959-1459
E-mail: elizmarkova@yahoo.com

Mikhail O. Efimov, *Candidates for a degree of Cand. Sci. (Eng.) of the Chair of Science named after V.M. Finkel',* Siberian State Industrial University
ORCID: 0000-0002-4890-3730
E-mail: moefimov@mail.ru

Сведения об авторах

Юрий Федорович Иванов, *д.ф.-м.н., профессор, главный научный сотрудник,* Институт сильноточной электроники Сибирского отделения РАН
ORCID: 0000-0001-8022-7958
E-mail: yufi55@mail.ru

Владимир Викторович Шугуров, *научный сотрудник лаборатории плазменной эмиссионной электроники,* Институт сильноточной электроники Сибирского отделения РАН
ORCID: 0000-0001-6148-9442
E-mail: shugurov@inbox.ru

Антон Дмитриевич Тересов, *старший научный сотрудник лаборатории плазменной эмиссионной электроники,* Институт сильноточной электроники Сибирского отделения РАН
ORCID: 0000-0002-5363-0108
E-mail: tad514@sibmail.com

Елизавета Алексеевна Петрикова, *младший научный сотрудник лаборатории плазменной эмиссионной электроники,* Институт сильноточной электроники Сибирского отделения РАН
ORCID: 0000-0002-1959-1459
E-mail: elizmarkova@yahoo.com

Михаил Олегович Ефимов, *соискатель степени к.т.н. кафедры естественнонаучных дисциплин им. проф. В.М. Финкеля,* Сибирский государственный индустриальный университет
ORCID: 0000-0002-4890-3730
E-mail: moefimov@mail.ru

Contribution of the Authors

Yu. F. Ivanov – scientific guidance, formation of the basic concept, goals and objectives of the study.
V. V. Shugurov – writing the text, obtaining and analyzing the data, reviewing publications on the article topic, obtaining data for analysis.
A. D. Teresov – obtaining and analyzing the data, finalizing the text.
E. A. Petrikova – analysis of the results of electron microscopic tests.

M. O. Efimov – conducting microhardness tests, data analysis.

Вклад авторов

Ю. Ф. Иванов – научное руководство, формирование основной концепции, цели и задачи исследования.
В. В. Шугуров – написание текста рукописи, получение и анализ данных, обзор публикаций по теме статьи, получение данных для анализа.
А. Д. Тересов – получение и анализ данных, доработка текста.
Е. А. Петрикова – анализ данных электронно-микроскопических исследований
М. О. Ефимов – проведение испытаний на микротвердость, анализ данных.

Received 20.07.2022
Revised 20.11.2022
Accepted 29.03.2023

Поступила в редакцию 20.07.2022
После доработки 20.11.2022
Принята к публикации 29.03.2023